



AHEAD Workpackage 8
JRA X-ray Optics

Deliverable D8.5 - D39

**Characterization of master high resolution XOU
for test performed at PANTER facility.**

Written by	Carlo Pelliciani (MPE)	
Checked by	Vadim Burwitz (MPE)	
Distribution List	AHEAD Management Team Vadim Burwitz WP8.0, WP8.1, WP8.3 Dick Willingale WP8.1 Rene Hudec WP8.1 Daniele Spiga WP8.1, WP8.2	
Distribution Date	Draft Version Final Version	Jan 10, 2018 May 25, 2018



Contents

1	Introduction	3
2	The PANTER X-ray test facility	3
2.1	The beam line	3
2.2	The X-ray sources	4
2.3	Detectors	5
2.3.1	TRoPIC	6
2.3.2	PIXI	6
2.3.3	PIXI and TRoPIC comparison	6
3	The coordinate system	6
3.1	Thin lens effect of the finite source distance at Panter facility with Wolter type optics	7
3.1.1	Alignment of Panter facility with modular optics.	8
3.2	Stepper Motor and Hexapod Accuracy	9
4	Optics description	9
5	Setup for MM-25 and MM-27	11
6	In air pre-alignment with visible light (laser)	12
7	Mask alignment under X-ray beam	13
8	MM-0025: alignment and Measurement test campaign	15
8.1	MM-0025: Pitch and Yaw scan	15
8.2	MM-0025: TROPIC and PIXI Focus search	17
8.3	MM-0025: TROPIC and PIXI azimuthal scan	19
9	MM-0027: Alignment and Measurement test campaign	20
9.1	MM-0027: Pitch and Yaw scan	20
9.2	MM-0027: focus search with PIXI and TROPIC	21
9.3	MM-0027: azimuthal scan with PIXI and TROPIC	23
10	Results	25
11	Summary	26

Abstract

To be able to verify the functionality of BEaTriX test facility a “master” SPO has to be precisely characterized at the PANTER X-ray test facility. For the purpose two state of the art SPO optics specifically made for the Assembly, Integration, and Testing (AIT) effort to co-align mirror modules in ATHENA mirror assembly were provided to PANTER for characterization. The characterization of these modules also allowed us to investigate the quality of these optics as a “master optic” for later verifying BEaTriX.

1 Introduction

In the document we describe the setup and we report the results of the measurement of the Mirror Modules MM-0025 and MM-0027. MM-0027 and MM-0025 are optics based on the pores optics technology. They are made of two similar X-ray Optical Units (XOU). Only the outer one of each MM has been characterized. Two different test campaigns have been prepared to measure each mirror module using the same setup. Each test campaign engaged the PANTER team for 2 weeks included final setting up, measurements and preliminary data analysis.

Once the MM has been mounted and aligned under visible light (laser) the chamber is closed and the air evacuated until the vacuum is lower than 10^{-6} mbar. Then the flux of the beam reflected by the optics is maximized tilting the mirror module itself (pitch and yaw). Once the optics has been aligned a focus search and an azimuthal scan of the mirror surface are performed.

2 The PANTER X-ray test facility

The PANTER X-ray test facility is primarily used to characterize X-ray optics for astronomy [6]. For this task the facility was built in 1977 and constantly updated over the years. Historically, the facility was designed for ROSAT, extended for XMM-Newton, and upgraded in 2012 for the IXO and ATHENA.

The PANTER facility is specialized in characterization of X-ray optics in general but for every test campaign a new setup is usually required to fit the mechanical interface, the focal distance and other physical parameters that are necessary to fully characterize the optics.

The PANTER test facility main components are X-ray sources, a 120 m vacuum pipe with a diameter of 1 m, a primary big chamber and a small movable one (figure 1). Those chambers have been added and modified during the years to fit the requirements of the incoming experiments. Therefore the optical benches allow a large range of configurations. In order to characterize X-ray optics, the PANTER X-ray test facility provides a set of X-ray sources and detectors. X-ray sources and detectors are mostly in-house developments or at least optimized in collaboration with the MPE.

2.1 The beam line

In order to simulate an in orbit configuration to characterize an X-ray telescope an infinite point source distance and a full illumination of the telescope will be the ideal configuration. By placing the X-ray source at a distance that is large compared to the focal length of the optics, the PANTER facility provides in first approximation such a collimated and large scale X-ray beam. An aerial photo of the facility are shown in Fig. 7.

The overall optical beam-path of the PANTER X-ray test facility provides a total beam path length of up to 145 m. This is realized with fixed parts and a movable extension. The fixed part, shown schematically in Fig. 7, is made up of the vacuum tube (length 122 m and diameter 1 m) and an instrument chamber (length 12 m and diameter 3.5 m) that houses the optics and the focal plane instruments. At one end of the fixed part various X-ray point sources can be connected to the tube. With this configuration, optics with a focal length up to 12 m can be characterized.

Recently, the PANTER was upgraded [1] with:

- an extension chamber (figure 1) that can be connected to the instrument chamber in order to characterize optics with a focal length ≥ 10 m. Originally designed for IXO, an X-ray telescope with $f = 20$ m proposed as a joint effort by NASA and ESA, this extension enables also the possibility to measure ATHENA type optics. This extension consists of a small vacuum tube (5 modules of length 2 m and diameter 0.25 m, see

Fig. 2) and an extension chamber (length 3 m and diameter 1.2 m, see Fig. 3) where the PIXI detector (position sensitive, $20 \mu\text{m}$) can be mounted.

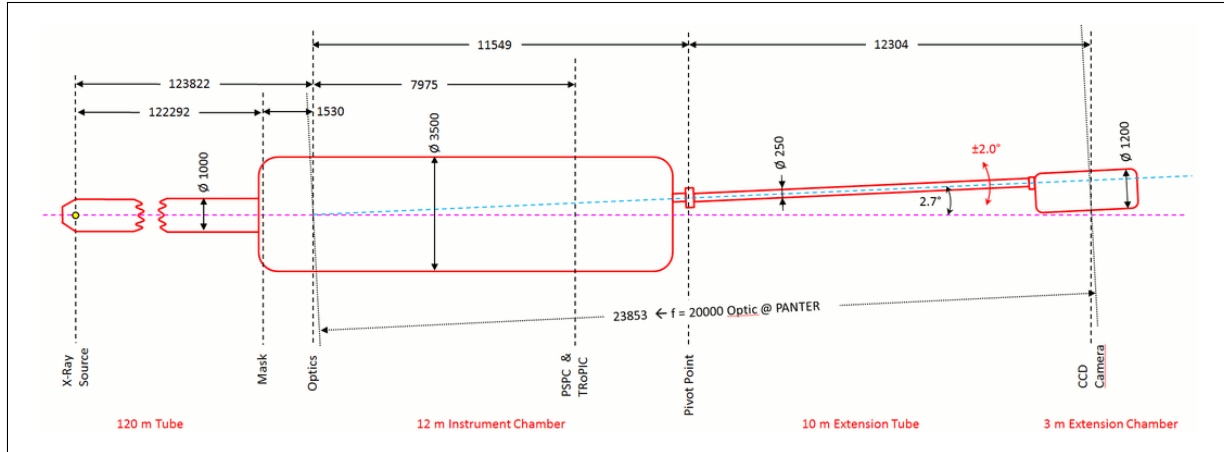


Figure 1: Sketch of the Panter beam line with tank-e implemented.

- a two meter optical bench has been implemented at the end of the 1 meter tube (figure 4). This new configuration allows the measurement of a 12 meter focal length without using the tank-extension. A sketch is reported in figure 4. This configuration is necessary in those cases in which the reflection is not fitting with the mechanical configuration Big Chamber + Tank-e¹. The 2 meter optical bench is equipped with a rail system with up to 5 carriage on which can be mounted 2 hexapods and 1 or 2 axis translator stages in order to setup a complete optical system. Not less important, this configuration permits to analyze optics using both both PIXI (position sensitive, $20 \mu\text{m}$ pixel resolution) and TRoPIC (energy and position sensitive, that can acquire images with different spatial resolution: 75, 40 and $25 \mu\text{m}$)



Figure 2: On the left the fixed large instrument chamber. On the right the extension tube.

Figure 3: Extension vacuum chamber to measure optics with a focal length $>10 \text{ m}$.

2.2 The X-ray sources

A more detailed description of the X-ray source is given in a previous applicable document [6].

To characterize X-ray telescopes on earth, an astronomical like X-ray source is necessary to be used as standard candle. This means in theory a point like source at infinite distance with infinitesimal energy resolution. In practice we have to use finite distances and finite source diameter that introduce extra small angular divergence during the mirror characterization (1 arcsec).

At PANTER X-ray tubes are used to produce X-rays. Technically an X-ray tube consists of a cathode (filament of Tungsten), which emits electrons and an anode (a target of a certain material) that collects these electrons.

¹Tank extension

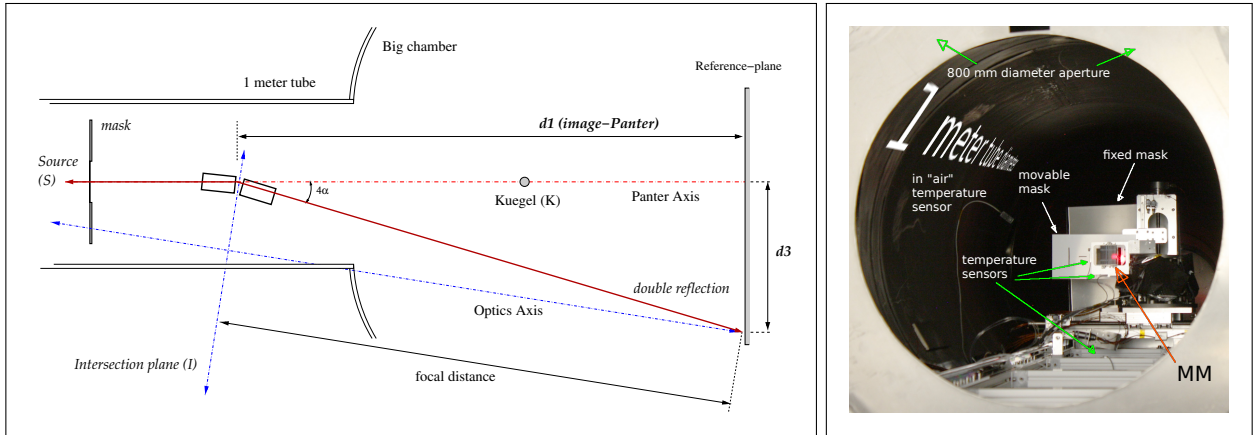


Figure 4: On the left: Draw of the mirror module in the tube view from the TOP. In this case, the beam is reflected in the Pantolsky side, i.e. opposite to the Tank-e direction. On the right: picture of the optical bench implemented in the one meter tube. Hexapod, MM and masks are visible.

Vacuum is needed in order to increase the mean free path length of the electrons. A high voltage power source U_{HV} is connected across cathode and anode to accelerate the electrons. The electron flux is regulated with the heat voltage U_{Heat} .

The spot size of the X-ray source is crucial characterizing the point resolution of the telescope. The size of the PANTER X-ray source has to be small compared to the point resolution of the telescope, i.e the angle from which is view the spot size has to be small compared to the point resolution of the telescope. The spot size can be influenced by various processes (e.g. a focused electron beam, apertures, a tilted target).

A smaller spot image in the Wald-Pantolsky direction is achieved by using a focusing Wehnelt voltage. The relationship between Wehnelt voltage and spot shape is under characterization (preliminary results reported in figure 5) but in any case the spot is smaller than one millimeter. This configuration contributes to increase the resolution of about 1 arcsec (to be added quadratically to the expected resolution of the mirror). A monochromatic X-ray beam can be achieved by using the characteristic fluorescence lines together with appropriate filters to reduce the Bremsstrahlung continuum.

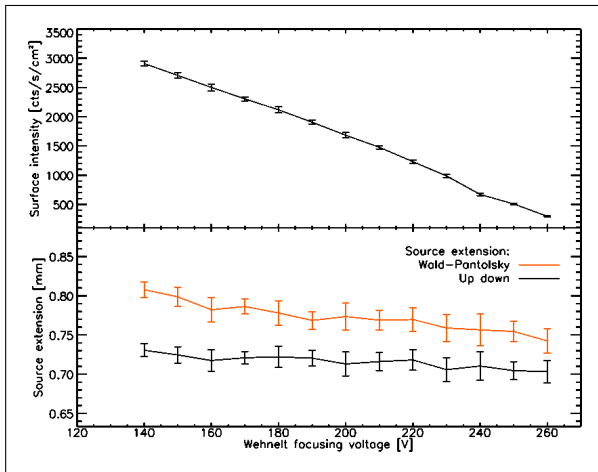


Figure 5: Spot size for Al-K α as a function of the Wehnelt voltage.

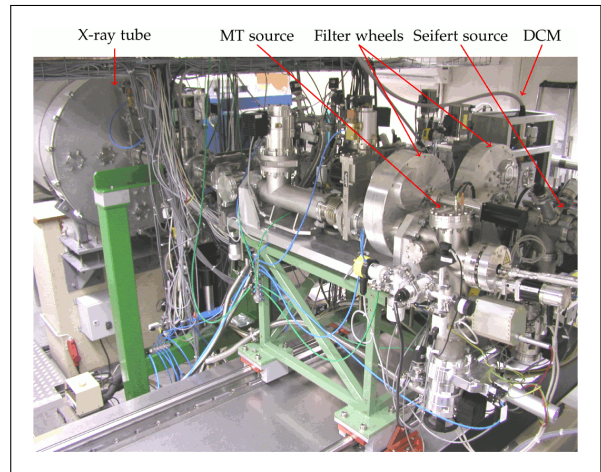


Figure 6: The PANTER X-ray sources. The sources can be connected individually to the beam line.

2.3 Detectors

In this section we give a short description of the detectors used during the test campaigns: TRoPIC and PIXI .

2.3.1 TRoPIC

The TRoPIC [4] detector is a small version of the one used for the eROSITA mission. It is designed to provide an high QE for the energy range from 0.1 keV to 10 keV. The back-illuminated CCD with a frame store region is coated with an Aluminum layer to absorb optical and UV light. The depletion region provides an high QE up to 10 keV [3]. Due to the low temperature $T = -100^{\circ}\text{C}$, which is achieved by liquid nitrogen (LN_2) cooling, the detector noise is low and TRoPIC can be used as spectroscopic detector. When using TRoPIC as spectroscopic detector similar to a single photon counter (i.e. count rates $< 1 \text{ cts frame}^{-1} \text{ pixel}^{-1}$ to prevent pile up) a pixel size of $75 \mu\text{m}$ can be using sub pixel informations improve the spatial resolution to $25 \mu\text{m}$ [2].

2.3.2 PIXI

The commercial CCD PIXI [5] is designed as soft X-ray imager up to 5 keV. The back-illuminated detector provides also the possibility to operate it in vacuum in the optical (e.g. optical stray light measurements). With a pixel size of $20 \mu\text{m}$ it is ideally suited for imaging with high spatial resolution at high count rates (i.e. integrating signals at the expense of losing the energy information) in the soft X-ray regime.

2.3.3 PIXI and TRoPIC comparison

The software related to TRoPIC gives the possibility to analyze the data as a function of energy and/or position. In this condition is possible to separate the fluorescence line from the bremsstrahlung. In fact, despite of the filter used, the bremsstrahlung component is still quite strong. For example it can be 30% of the total during standard operational, i.e. Al target with 5 kV acceleration voltage. PIXI is only position sensitive and it collects the charge in a interval range set by the user. During the acquisition, the photon energy information is lost and the analysis cannot be compared directly with TRoPIC unless a strongly monochromatic source is used. However, PIXI has a better spatial resolution ($20 \mu\text{m}$) and the acquisition time is 60 time faster (1 minutes instead of 1 hours). Another advantage of the PIXI is the portability. In fact a simpler cooling system can be used to cool down the detector, instead of the more complex setup necessary for TRoPIC. In this report we acquired with both detectors and differences are also reported.

3 The coordinate system

At Panter X-ray facility are in use an absolute and a temporary coordinate systems:

- The absolute reference system is reported in figures 7 and 8. It is in agreement with the left-handed coordinate system.
 - translation on: $+X = \text{Pantolsky} / -X = \text{Wald}$
 - translation on $+Y = \text{Top} / -Y = \text{Bottom}$
 - translation on $+Z = \text{towards detector (Küche)} / -Z = \text{towards to the source (Quelle)}$
- Temporary reference system. The axes orientation are belonging to the optics (for example see see figures 9):
 - Tilt system = Pitch: positive when the exiting surface of the optics start to point toward the ground.
 - Rotational System = Yaw: the rotation is around the vertical axis Y and it is positive in counter clock wise direction.
 - Linear Translator (on which Hexapod or other rotary/tilting systems are mounted):
 - * translation perpendicularly to the beam direction, positive towards Pantolsky (+Y).

In Fig. 8 the PANTER coordinates that will be used henceforth are sketched:

- The optical axis is defined with the X-ray source and the in focus point image of the optic, here called the Z-axis with Z increasing from the mirror to the detector. In general this axis coincides with the PANTER's geometrical axis which is defined by the 122 m vacuum tube.
- At the PANTER $+X$ is toward *Pantolsky* direction. The origin of the coordinate system is in general set at the intersection plane of parabola and hyperbola mirror and the optical axis.
- The Y-axis defines the up-down coordinate with increasing values toward the up direction.

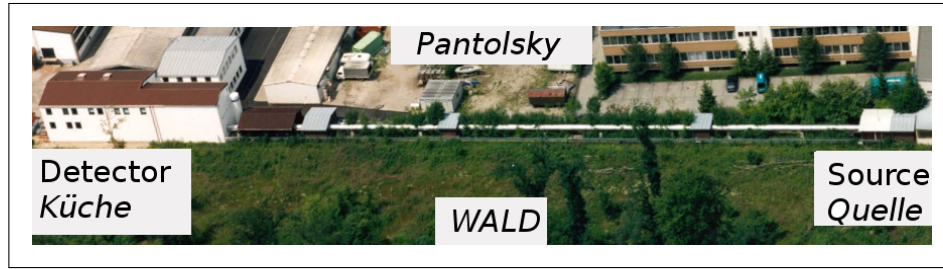


Figure 7: Panter reference system. For historical and practical reason the words such as Küche (kitchen), Quelle (Source), Wald (forest) and Pantolsky (former factory) represent an absolute reference system.

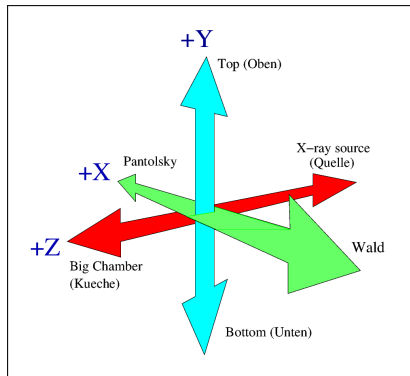


Figure 8: Left hand XYZ coordinate system.

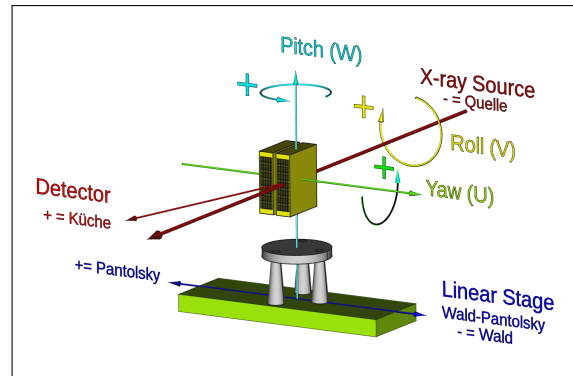


Figure 9: Yaw and Pitch axes for SPO optics.

Beside, the X-Y-and Z-coordinates two further degrees of freedom, two rotation angles, are necessary to characterize mirrors (figure 9):

- Rotation angle y or Pitch as seen from above.
- Tilt angle x / Yaw as seen from the Wald side.

Usually the Yaw is aligned along the radius of the optics, meanwhile Pitch is aligned with the tangent to the mirror. In any case the configuration can be changed depending on the optical system or the convention adopted by the users.

A rotation about the Z-axis can be theoretically defined but is in general not necessary as Wolter optics are rotationally-symmetric and a rotation about the Z-axis is equal to a rotation of the mirror around its symmetry axis. Adding a collimator to this set-up, the here defined coordinate system can be maintained if the optical axis of the collimator coincides with the system optical axis, defined by the X-ray source and mirror, here the Z-axis.

3.1 Thin lens effect of the finite source distance at Panter facility with Wolter type optics

Because of the finite Source S_p at Panter and because of the thin lens behavior of a Wolter type optics, the image or the effective focal length can be calculate using the following formula and its derivatives:

$$\frac{1}{f} = \frac{1}{s} + \frac{1}{i} \Rightarrow i = \frac{sf}{s-f} \text{ and } f = \frac{si}{s+i} \quad (1)$$

where we have:

f focal distance of the thin lens;

s source distance;

i image distance;

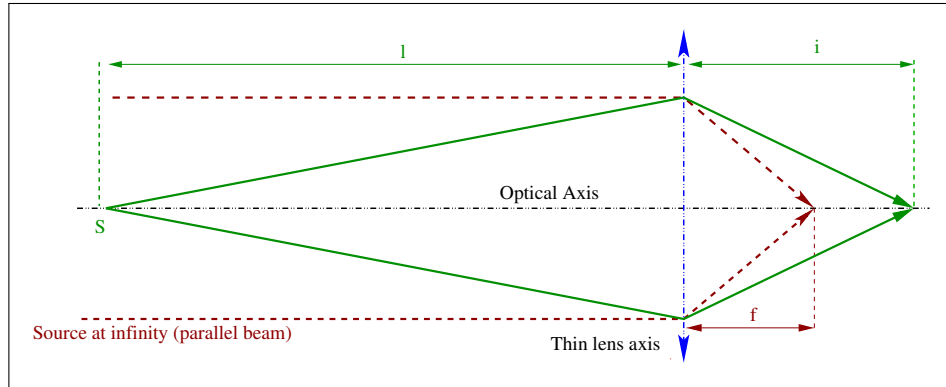


Figure 10: Finite source distance effect on the image determination. The image spot is focused at a larger distance compared to the focal length of the optics itself f . According to the theory, the Wolter type telescope has a behavior as like a thin lens system $\left(\frac{1}{f} = \frac{1}{s} + \frac{1}{i}\right)$.

3.1.1 Alignment of Panter facility with modular optics.

In this paragraph we report the formulas used to obtain the correct image distance i calculated from the intersection plane. The procedure is applied on the figure 11 that is similar to figure 10 but aligned with the PANTER facility axes.

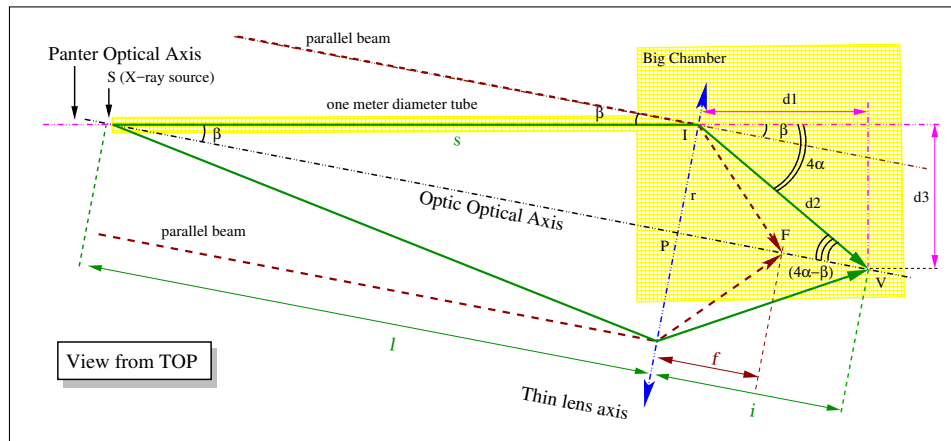


Figure 11: Top view of a schematic of the PANTER X-ray facility. This graph illustrates the concept of the alignment between a modular optics and the PANTER facility. The yellow filled area represents the 120 long meter tube and the big-chamber. Parameter definitions are reported in table 2.

The i quantity can be calculated with two methods:

1. With the Pythagoras theorem:

$$i = \sqrt{d_2^2 - r^2} \quad (2)$$

2. Calculating β and projecting h on the Optical axis

$$\beta = \arctan\left(\frac{r}{l}\right) \quad (3)$$

$$i = d_2 \cos(4\alpha - \beta) \quad (4)$$

Because the angles are small, in first approximation or during a very preliminary alignment, it is possible to align the system calculating the variable q :

$$d_1 = d_2 \cos(4\alpha) \quad (5)$$

Table 2: Definition of the parameter relative to figure 11. The kugel represents tilt/rotation point of the telescope workbench.

f	real focal distance of the mirror	α	reflection from the single optical component; 4α represents the reflection from a complete module.
s	Panter source distance $s = \overline{SI} \approx 119.4$ m	β	angle from which the optics radius is seen from the source
i	Panter image distance	$d1$	the projection of $d2$ on the Panter optical axis
r	radius of the mirror module (≈ 737 mm)	$d2$	distance measured at the Panter facility during the test campaign, e.g 13 m. Also called hypotenuse.
l	Distance between the Mirror Module Intersection Plane and the PANTER X-ray source source. $l \approx 119.4$ m .	$d3$	Distance between direct and reflected beam in the PANTER coordinate system.

The discordance between i and q is a factor of -0.0003 . For example, if $h = 13$ m, i will be ≈ 4 mm larger than q .

$$i \approx \Delta i = \frac{\cos(4\alpha - \beta) - \cos(4\alpha)}{\cos(4\alpha)} \approx d_1 + 4.3 \quad (6)$$

with $\alpha = 3.51^\circ$ (for construction) and $\beta \approx 0.32^\circ$ (calculated).

3.2 Stepper Motor and Hexapod Accuracy

We list the stepper accuracy for each Hexapod, for the translation stage and rotary and tilt stages. For more details look for the official documentation. Some extra note in the following list.

- Little Hexapod (811.DV), max 5 kg on vertical, 2.5 in other orientations.
- Linear translation stages: min. step = $1.25 \mu\text{m}$
- Tilt and Rotary stages: min step = $0.9''$

Table 3: Hexapod performances

Hexapod		Linear movement						Angular movement ($\text{arcsec}/\mu\text{rad}$)					
stage	description	Range (mm)			min step (μm)			Range ($^\circ$)			min step (μm)		
		X	Y	Z	δX	δY	δZ	X (U)	Y (V)	Z (W)	θX (U)	θY (V)	θZ (W)
PI 811.D2V	Little Hexapod (5 Kg)	± 17	± 16	± 6.5	0.5	0.5	0.2	± 10	± 10	± 21	0.7/3.5	0.7/3.5	0.7/3.5
PI 824.G2V	Grosse Hexapod (5 Kg)	± 22.5	± 22.5	± 12.5	0.3	0.3	0.3	± 7.5	± 7.5	± 12.5	0.7/3.5	0.7/3.5	0.7/3.5

Table 4: 3 axis motorized stages TANK-e

Axis	Instrument	Directions	1 step =	1 mm =
1.1	PIXI	-Quelle + Küche	$8.00 \mu\text{m}$	125 steps
1.2	PIXI	-Pantolsky + Wald	$1.25 \mu\text{m}$	800 steps
1.3	PIXI	-rauf + runter	$1.25 \mu\text{m}$	800 steps

Table 5: Detectors

1 Pixel TRoPIC	$75 \mu\text{m}$
1 Pixel PIXI	$20 \mu\text{m}$

4 Optics description

Two X-ray Optical Units (XOU), manufactured with the silicon pore optics technology (SPO) and with the same nominal radius are mounted on the same frame. Only the outer module will be measured. Table 3 reports

the main parameters of the optics, such as focal length and radius. In the figure 12 two view of the MM-0027 are shown. The optics is assembled in the mechanical interface that permits to mount the mirror module on the hexapod.

Table 6: **Nominal** parameters of the MMs. Radius (r) and focal length (f).

MM	XOU	r (mm)	f (mm)	Comments
MM-0027	XOU-0048	737	12000	-
MM-0025	XOU-0041B	737	12000	-

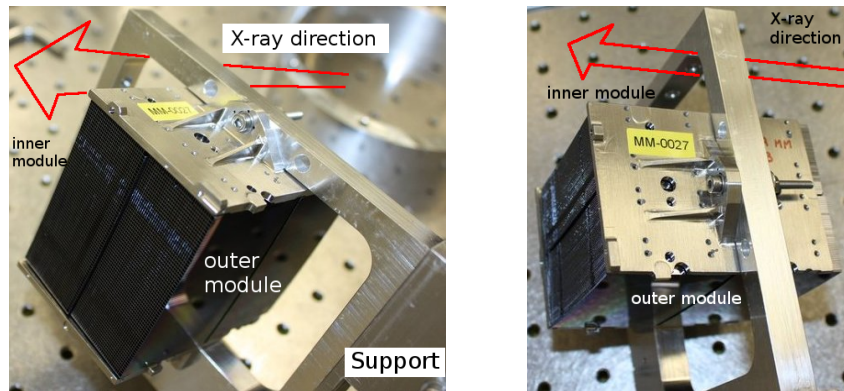


Figure 12: Pictures of the MM#2 MM-0027 inserted in the mechanical interface for the hexapod mounting. MM-0025 has been assembled using the same setup and configuration.

5 Setup for MM-25 and MM-27

In this paragraph a short description of the setup is given. A sketch of the top view measurement setup is reported in figure 13. From the left of the before mentioned sketch we can see: the fixed mask, the movable mask, the mirror module (the hexapod is not designed) and the reference plane on which the X-ray beam is focused. This reference plane is perpendicular to the incoming beam and not to the axis of the MM. This means that the real PSF is 0.2% smaller (this correction is indeed negligible) than the acquired images.

The tables 7 and 8 report the distances between source, optics and other components useful for data acquisition and analysis.

Pictures 15 shows a mechanical draw of the mask.

In figure 14 are reported two pictures of the MM-0027 assembled on the hexapod and installed in the 1 meter tube.

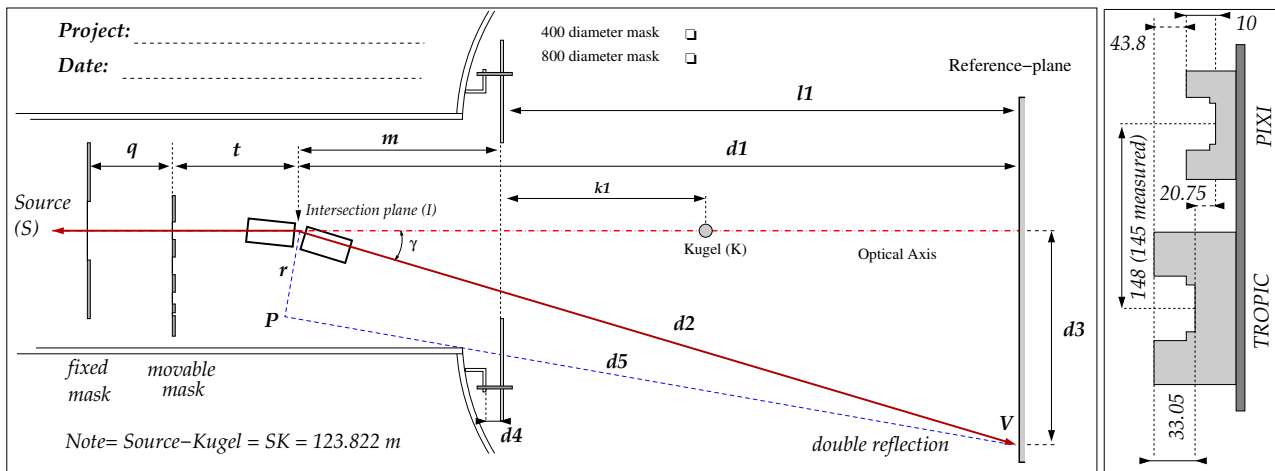


Figure 13: Setup view from the Top. On the right side PIXI and TROPIC dimensions.

The previously mentioned main components are here described in details:

1. The X-ray source can be approximated to an ellipsoid with the major-axes smaller than 1 mm. It is located at the beginning of the vacuum tube, at about 119.4 meters from the intersection plane of the optics. At this distance, the X-ray source introduces an extra-broadening on the MM resolution ≈ 1.5 arcsec to be subtracted quadratically from the final data.
2. A fixed mask is mounted between source and movable mask. Without the fixed mask, direct beam coming from the source will overlap the beam reflected from the MM itself (figure 14).
3. A second mask (figures 14 and 15) can be moved in the YX plane, perpendicularly to the beam. The mask has several apertures that permits choose to irradiate the optics with A = 100%, B = 90% or C = 5% of the full acceptance mirror module windows. The D=10% aperture is designed to analyze few planes but was not used because the transversal range is limited by the radius of the vacuum tube walls.
4. The Mirror Module is mounted on one side of the hexapod PI-824.
5. The hexapod has been covered by a IR reflector material to protect the optics from IR radiation generated by the electronics and the motors of the hexapod itself.
6. Temperature sensors have been implemented to monitor any temperature gradient. They are glued or screwed on optics holder, on the hexapod and on the rail, see figure 14 and ??

Table 7: Setup distances from the CCD of PIXI during MM0025 test campaign (see figure 13).

MM-0025: Setup (mm)				
	before	after	fixed	
d1	13343	13263	q	440
d2	-	-	t	234 (237 measured)
d3	818	800	m	2840
d4	60	60	k1	1580
l1	10405	10405	\overline{SK}	123822
-	-	-	\overline{SI}	119400

Table 8: Setup distances from the CCD of PIXI during MM0027 test campaign (see figure 13).

MM-0027: Setup (mm)				
	before	after	fixed	
d1	13242	13249	q	440
d2	-	-	t	234 (237 measured)
d3	800	800	m	2840
d4	60	60	k1	1580
l1	10405	10405	\overline{SK}	123822
-	-	-	\overline{SI}	119400

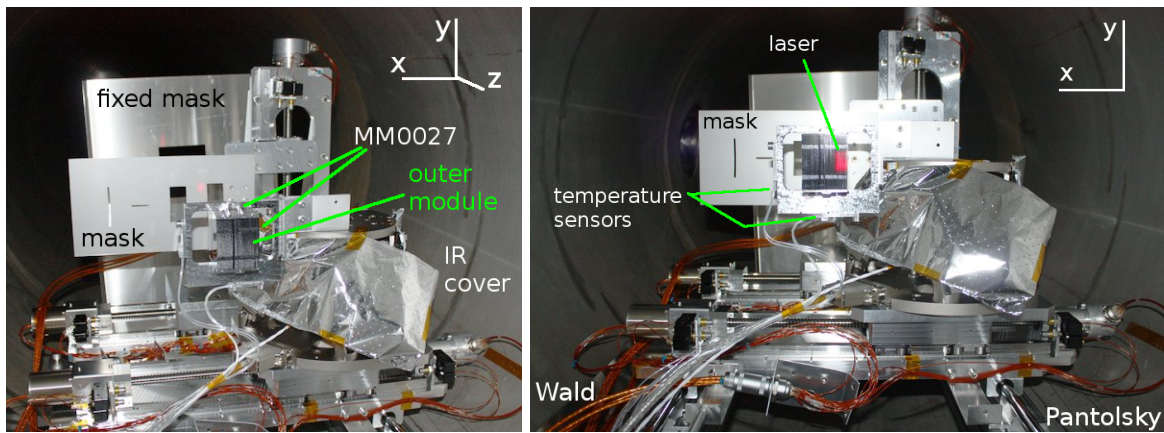


Figure 14: Two pictures of MM#2 (MM0027) mounted in the tube and ready or the X-ray measurement (of course only after pumping).

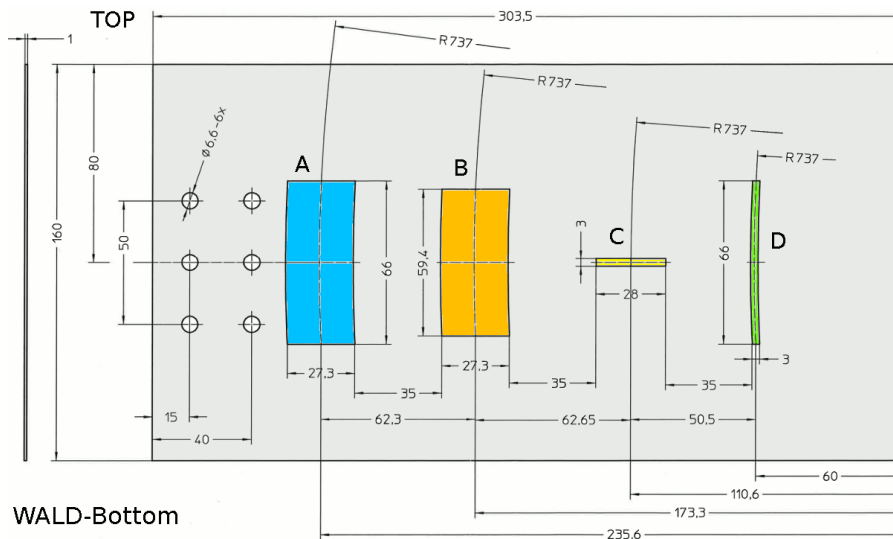


Figure 15: Mask dimensions.

6 In air pre-alignment with visible light (laser)

The laser pre-alignment is a procedure that permits to roughly align the optics with the X-ray source and the detector. A successful pre-alignment requires laser beam and X-ray source to be aligned on the same PANTER optical axis with an error of few millimeters. Then the procedure consists in to look for the double laser reflection from the Wolter mirror and finally to move the detector in such position. Because of the small structure of

the MM, instead of a small spot a diffraction pattern will be visualized. The procedure is repeated for both mirrors modules. The distances between optics and detector (figure 13) are recorded before and after the X-ray measurement as reported in table 7 and 8.

In Air alignment procedure:

- the camera is positioned near the expected focus position, i.e. calculated with nominal parameters:

- Input nominal parameter (from table 6):

f : focal length = 12.0 m;

r : radius = 737 mm;

$s \approx 1$: source distance = 119.4 m.

- Use of the thin lens formula (equation 1) to calculate the expected image distance i :

$$d_5 = i = \frac{f \cdot s}{s - f} \approx \frac{12 \cdot 119.4}{119.4 - 12} \approx 13.340 \text{ m} \quad (7)$$

$$d_2 = \sqrt{(d_5^2 - r^2)} \approx 13.320 \text{ m} \quad (8)$$

then:

$$d_1 = d_2 \cos(4\alpha) \approx 13.295 \text{ m} \quad (9)$$

$$d_3 = d_2 \sin(4\alpha) \approx 815 \text{ mm} \quad (10)$$

- Laser alignment:

- the MM is moved under the laser beam (figure 14):

- the MM is tilted (YAW and Pitch) in order to see the double reflection spot;

- the detector is moved on the double reflection spot (figure 16). The diffraction pattern is a consequence of the interference of the laser with the XOU mechanical structure. during the laser alignment several spots appear because of the multiple reflection inside of the XOU. A important discrimination between the real focal spot and the multiple-reflections is that the focus doesn't change position with the rotation (PITCH) of the optics meanwhile single and multiple reflections do. X-ray will not be visible if the optics is aligned under a multiple reflections condition.

Using this procedure and with experience we are able to pre-align the optics with angular accuracy of few arcmin and move the detector in the right spatial position within few millimeters.

Without this pre-alignment the X-ray alignment will take days because it will be necessary to scan the entire focal plane and in the same time tilt the optics to see if any reflection occurs.

7 Mask alignment under X-ray beam

Two main alignment sequences have to be performed in vacuum before to proceed with the optics characterization:

- mask alignment,
- angular optics orientation (maximization of the flux during pitch and yaw).

In this paragraph we give a short description of the mask alignment after evacuation of the air under X-ray beam illumination. The mask, optics and detector are aligned only on the double reflected beam and not on direct beam.

Mask alignment concept: we move the the mask over the optics until the focal spot disappears indicating the relative position of the wall of the aperture compared to the mask itself.

- Starting point: the mask was previously aligned with the laser. Usually, the accuracy is between 5 and 10 mm.
- Aligment of the mask in vacuum under X-ray illumination. The mask alignment is necessary in order to know the position of the mask compared the one of the optics. A pre-alignment in visible light is performed, but the accuracy can be some millimeters up to 1 centimeter. Two method can be used to align mask and optics each other :

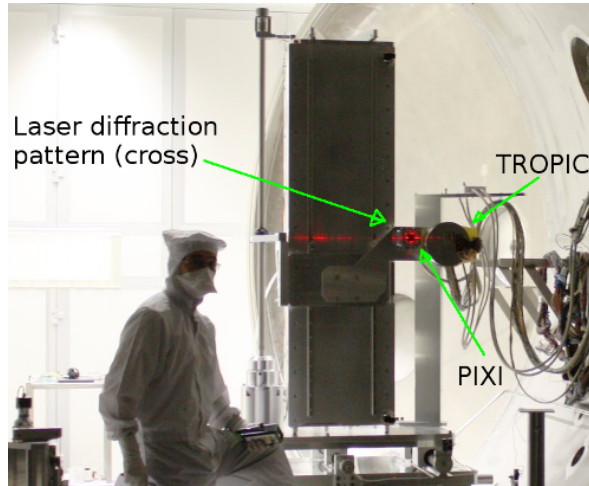


Figure 16: Focus search with the diffraction pattern produced by the laser. A good optical alignment is necessary to localize the reflected X-ray beam within few arcmin.

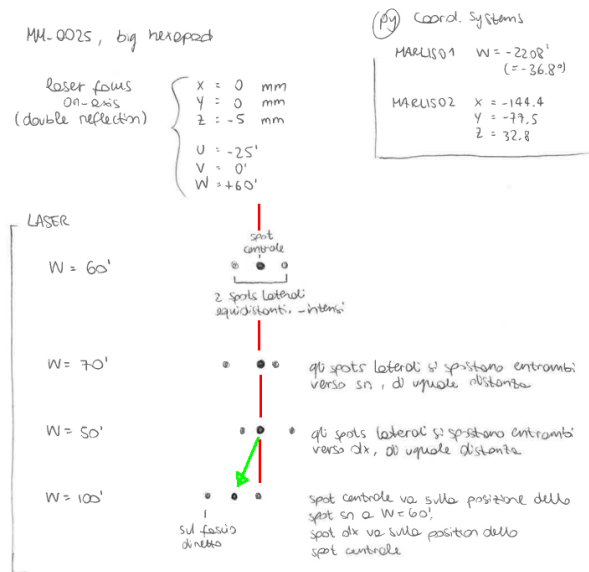


Figure 17: The double reflections (or 4α reflection) doesn't change position except in those case in which we have multiple internal reflections. A multiple reflection has been founded with a tilt of 1 degree (last position in the bottom).

1. this method is based on the fact that the convolution between 2 rectangular functions (aperture and MM) is a trapezoid or a triangle (this is the case in which the two rectangular functions have the same dimensions). The aperture is moved relative to the optics. The position of the aperture is given by the intersection of the non-parallel faces. Usually this method is the fastest and gives information about the reflectivity vs irradiated area.
2. this method consists to find the side of Mirror Module. The aperture is moved on the plane perpendicular to the x-ray beam, i.e. left and right, up and down until the flux of photons reflected by the optics is almost zero. The mask has to be positioned in middle of the positions where the flux is almost zero. This method permits to see check the border of the optics. This second method can be used in conjunction with first one, only to check the sides of the optics.

8 MM-0025: alignment and Measurement test campaign

We report the laser alignment procedure, the Yaw and Pitch scan measurement in order to optimize the position for the mirror module MM-0025. Finally then we perform the best focus search and the azimuthal scan with the 5% mask.

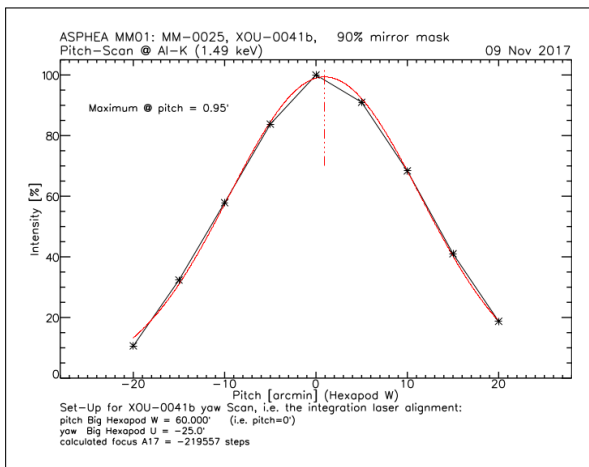
8.1 MM-0025: Pitch and Yaw scan

The Optics is rotated and tilted in order to maximize the flux first in Pitch and then in Yaw. The axis orientation is reported in figures 9. During YAW scan, the optics “fall” in the detector direction. During PITCH, optic rotates in CCW direction around the vertical axis.

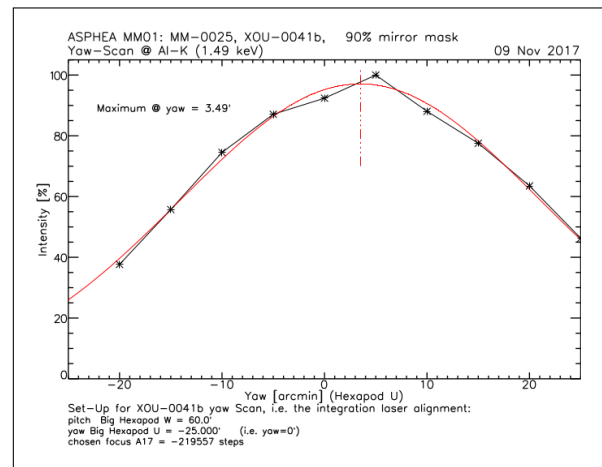
In this section we report the graph of pitch and yaw alignment obtained with PIXI and TRoPIC . Table 9 summarize the results. The values written between parenthesis represent the discrepancy with the laser alignment. In this test campaign, pitch and yaw are not significant because there is no direct comparison between the two optics. In fact, also if the setup used for the test campaign is the same, the mounting - dismounting procedure is not repeatable.

Table 9: MM-0025 pitch and yaw alignment. The value reported in the table are the absolute value read on the hexapod. The value between parenthesis represents the discordance with the pre-alignment (laser light).

Mirror Module	MM-0027			graph or images
Detector	PIXI (laser)	TRoPIC (laser)	(TRoPIC - PIXI)	
Pitch (arcmin)	+62.085 (0.95)	+62.11 (1.34)	+1.5''	fig. 18 and 19
Yaw (arcmin)	-19.300 (3.49)	-19.81 (4.28)	-30''	fig. 20



(a) Pitch scan.



(b) Yaw scan.

Figure 18: XOU-0041b of XMM-0025 pitch and yaw scan.

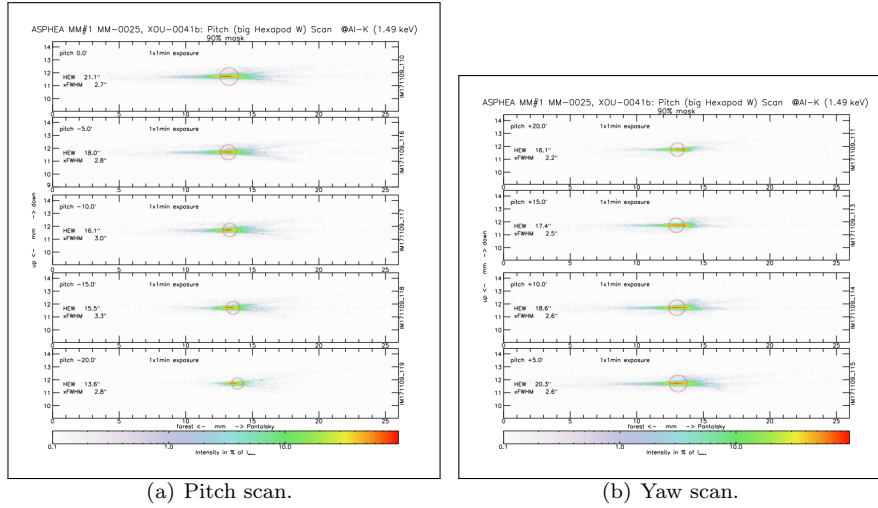


Figure 19: XOU-0041b of XMM-0025 pictures of the PSF during the pitch scan.

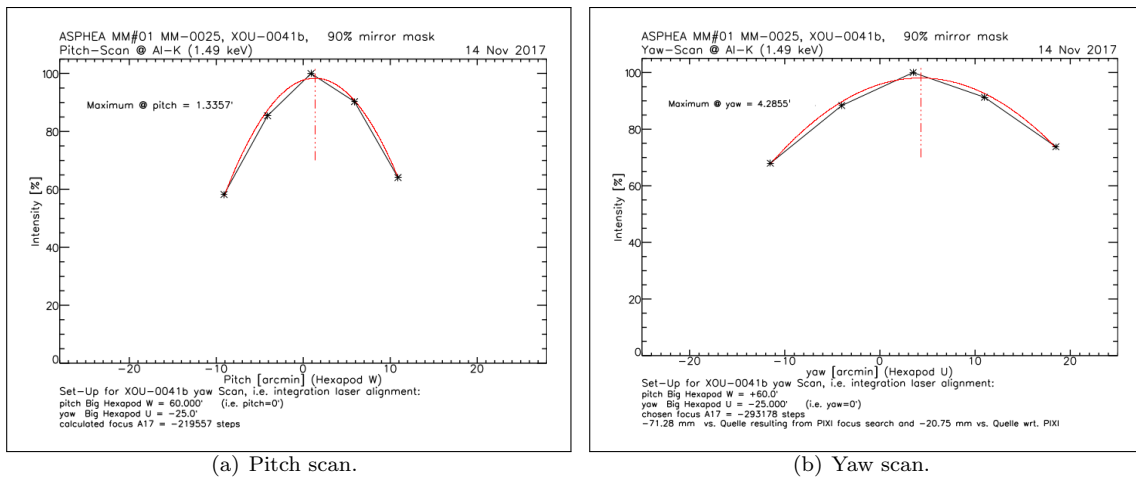


Figure 20: XOU-0041B (MM-0025) pitch and yaw scan.

8.2 MM-0025: TROPIC and PIXI Focus search

In this paragraph we report setting, graph and pictures of the data acquired during the focus search. At the PANTER x-ray facility, the focal distance is a parameter that is obtained from indirect measurement for this main reasons:

1. the beam generated by the PANTER facility is divergent and the obtained value has to be calculated with the thin lens formulas reported in section 3.1.
2. the stepper motors gives only relative movement and not absolute. The focal distance is obtained measuring with a laser distanziometer the distance between the detector and the intersection plane of the optics. The error is ≈ 5 mm. The reason is that the focal distance have a length approximatively 20 times bigger than the translator stage installed at PANTER . The motorized linear stage has a range of about 400 mm and it is installed on a manually movable rail system with a range of few meters and there is no direct measurement from detector to optics, i.e. a long linear encoder(!)².

The distance measured from the detector PIXI (CCD surface) to the intersection plane is:

$$d1 = 13263 \text{ mm} \quad (11)$$

corresponding to a step position of the source-detector linear stage Axis n.17:

$$A17 = -260515 \text{ steps} \quad (12)$$

From the information written above (eq. 11 and 12), the thin lens equation (eq: 1) and the setup (fig. 13) we obtained a focal length $f_{MM0025-pixi-fwhm}$ of:

$$f_{MM0025-pixi-fwhm} = 11940 \text{ mm} \quad (13)$$

Using the d1 written before and knowing the motor step positions (figures 21), we obtained the value of the focal length for different setup and as function of HEW and xFWHM (table 10).

Table 10: Results of the focus scan, after the mirror alignment. The results are obtained using the 90% mask. The contribution of the source has been subtracted from the xFWHM. In the other case the contribution is negligible.

MM-0025 (XOU-0041b): focus search using transversal FWHM (xFWHM)						
MM	Detector	Motor steps 1.25 $\mu\text{m}/\text{step}$	d2 (fig. 11) (mm)	HEW (arcsec)	xFWHM (arcsec)	Focal Length (mm)
MM-0025 XOU-0041b	PIXI	-260515	13288 \pm 3 mm	20.2	1.7	11941
	TRoPIC	-257329	13313 \pm 3 mm	24.3	1.7	11961

Table 11: Results of the focus scan, after the mirror alignment. The results are obtained using the 90% mask.

MM-0025 (XOU-0041b): Focus performances using HEW as focusing parameter						
MM	Detector	Motor steps 1.25 $\mu\text{m}/\text{step}$	d2 (fig. 11) (mm)	HEW (arcsec)	xFWHM (arcsec)	Focal Length (mm)
MM-0025 XOU-0041b	PIXI	-309778	13226 \pm 3 mm	20	4	11891
	TRoPIC	-358310	13186 \pm 3 mm	23.9	6	11858

The difference between the focal length obtained with the two detector is probably due the fact that PIXI is not energy sensitive. Reversely TRoPIC has a worse position accuracy. Because of those differences between the two instruments we cannot really prefer one of the two (see section 2.3 for more details). Moreover, for efficiency purpose, the tube settings used with the two detectors are slightly different (table 12). The focal length obtained using HEW as main parameter is reported in table 11 and it shows a shorter focal length.

²In the next future laser tracker system will be installed for sub millimeter accuracy measurements.

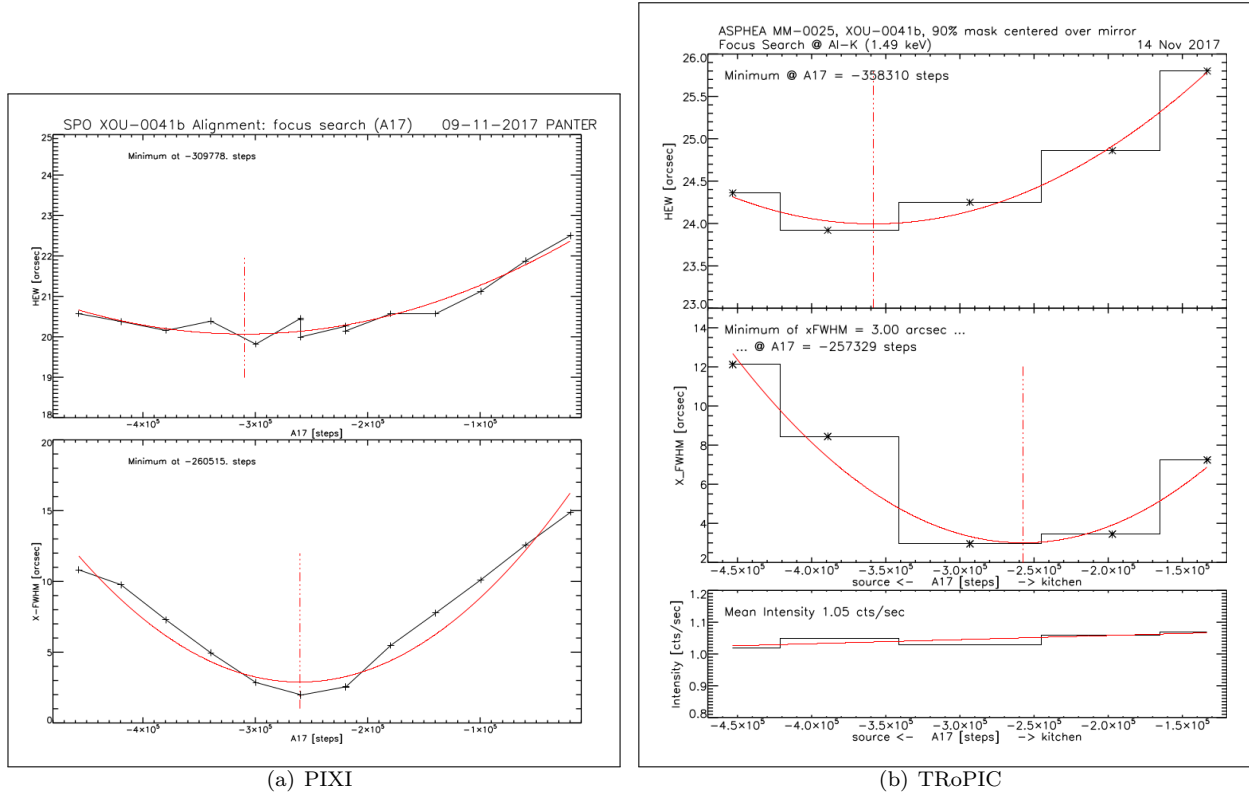


Figure 21: MM-0025-0041b: transversal FWHM (xFWHM) and HEW vs focal distance. 800 steps = 1 mm. TRoPIC and PIXI CCDs are 20.75 mm distance each other, equivalent to 16600 steps. Negative direction toward source. Setup in figure 13.

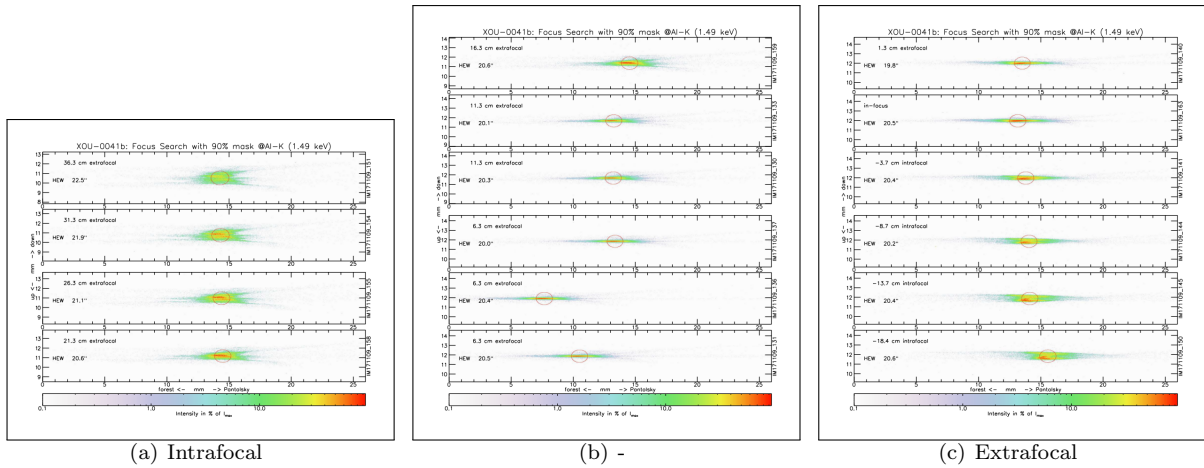


Figure 22: XOU-0041b of XMM-0025 pictures of the PSF during the focus scan. PIXI detector.

Table 12: X-ray tube value set during the MM-0027 focus search with TRoPIC and PIXI detectors.

Detector	Target	Filter	Fluorescence line [7]	kV	Focusing	Heating	figures
TRoPIC	Al	Al	Al-K = 1.486 keV	3	50 V	5.18 V	21(b)
PIXI	Al	Al	Al-K = 1.486 keV	5	50 V	8 V	21(a), 22

8.3 MM-0025: TROPIC and PIXI azimuthal scan

In this section we report graph and images acquired during the azimuthal scan. It consists in the acquisition of images and flux with a mask that cover only the 5% of the entire mirror module. The aperture is rectangular (see aperture C in figure 15).

The azimuthal scan with TRoPIC was repeated to confirm the big peak in the center of the optics. Large deformation are visible on the side of the optics itself.

The best recored HEW is 8.7 arcsec.

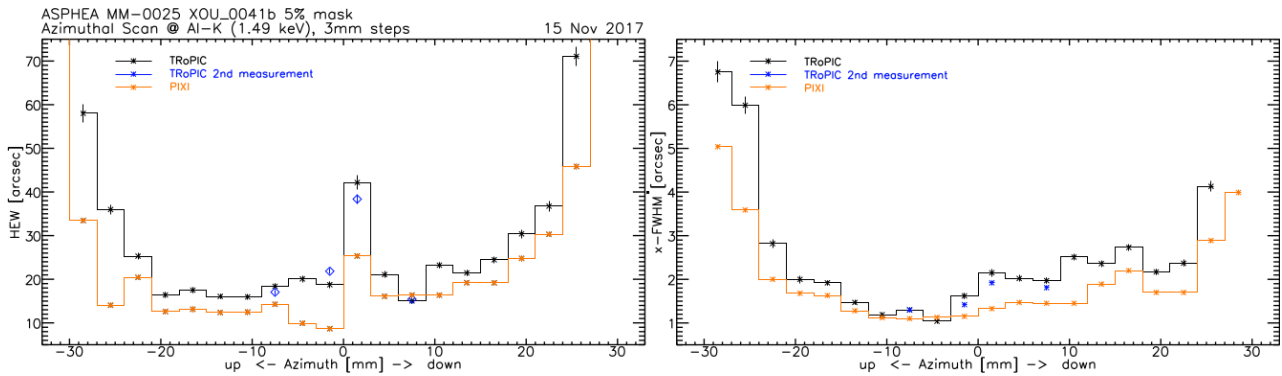


Figure 23: MM-0025. Azimuthal scan with 5% mask.

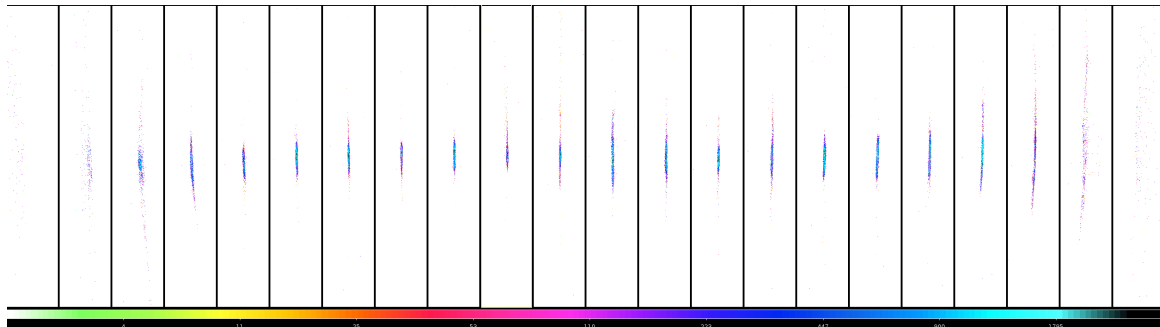


Figure 24: MM-0025, image of the PSF during the azimuthal scan with 5% mask. Detector = PIXI. Linear scale of the intensity.

9 MM-0027: Alignment and Measurement test campaign

We report the laser alignment procedure, the Yaw and Pitch scan measurement in order to optimize the position for the mirror module MM-0027. Finally then we perform the best focus search and the azimuthal scan with the 5% mask.

9.1 MM-0027: Pitch and Yaw scan

The Optics is rotated and tilted in order to maximize the flux first in Pitch and then in Yaw. The axis orientation is reported in figures 9. During YAW scan, the optics “fall” in the detector direction. During PITCH, optic rotates in CCW direction around the vertical axis.

In this section we report the graph of pitch and yaw alignment obtained with PIXI and TRoPIC . Table 13 summarize the results.

The values written between parenthesis represent the discrepancy with the laser alignment. In this test campaign, pitch and yaw are not significant because there is no direct comparison between the two optics. In fact, also if the setup used for the test campaign is the same, the mounting - dismounting procedure is not repeatable. Comparison between MM-0025 and MM-0027 is summarized in table 17

Table 13: MM-00278 pitch and yaw alignment. The value reported in the table are the absolute value read on the hexapod. The value between parenthesis represents the discordance with the pre-alignment (laser light).

Mirror Module	MM-0027			graph or images
Detector	PIXI (laser)	TRoPIC (laser)	(TRoPIC - PIXI)	
Pitch (arcmin)	+ 62.085 (1.19)	+62.1144 (n.d.)	2''	fig. 25 and 27
Yaw (arcmin)	- 19.3 (2.21)	-19.8147 (n.d.)	30''	fig. 26

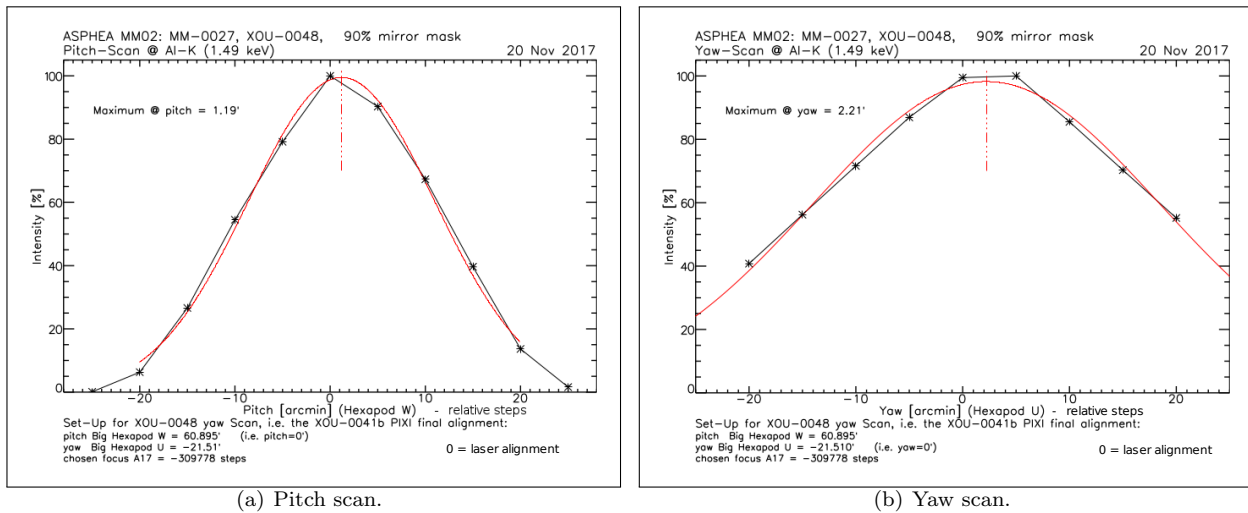


Figure 25: XOU-0048 (MM-0027) pitch and yaw scan. NOTE: the X scale reports the RELATIVE value used during the hexapod scan. The X=0 corresponds to the laser alignment The W and U values are the starting value of the hexapod.

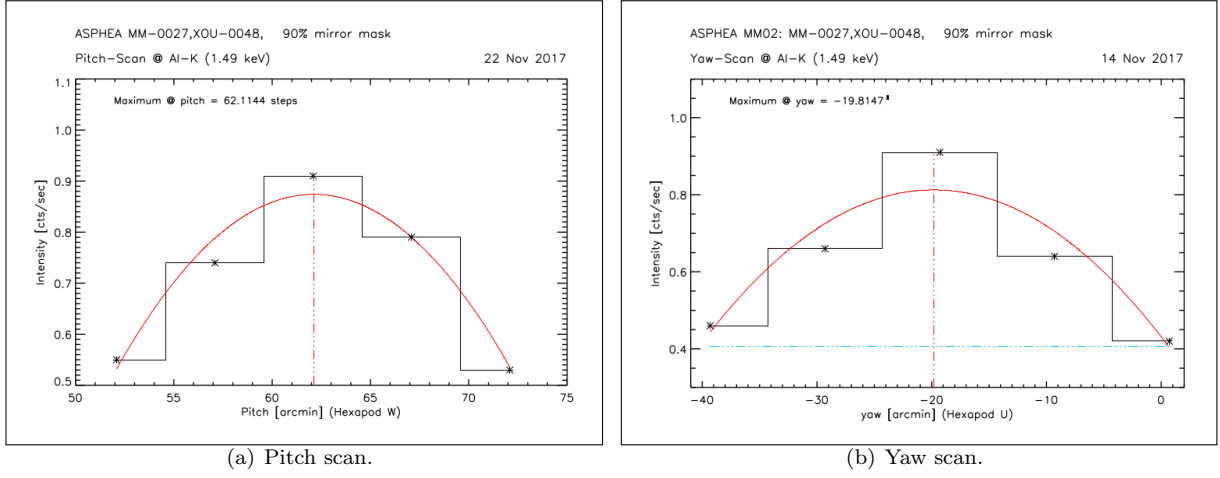


Figure 26: XOU-0048 (MM-0027) pitch and yaw scan.

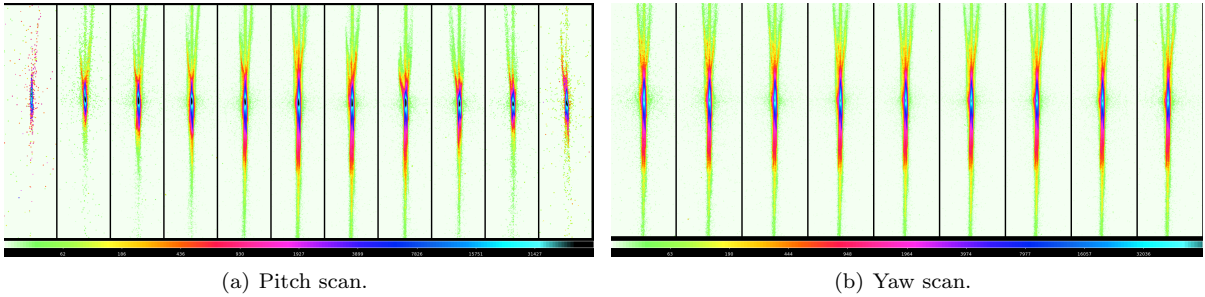


Figure 27: MM-0027: PIXI pictures of the PSFs acquired during Pitch and Yaw scan.

9.2 MM-0027: focus search with PIXI and TROPIC

In this paragraph we report setting, graph and pictures of the data acquired during the focus search. At the PANTER x-ray facility, the focal distance is a parameter that is obtained from indirect measurement for this main reasons:

1. the beam generated by the PANTER facility is divergent and the obtained value has to be calculated with the thin lens formulas reported in section 3.1.
2. the stepper motors gives only relative movement and not absolute. The focal distance is obtained measuring with a laser distanzimeter the distance between the detector and the intersection plane of the optics. The error is ≈ 5 mm. The reason is that the focal distance have a length approximately 20 times bigger than the translator stage installed at PANTER . The motorized linear stage has a range of about 400 mm and it is installed on a manually movable rail system with a range of few meters and there is no direct measurement from detector to optics, i.e. a long linear encoder(!)³.

The distance measured from the detector PIXI (CCD surface) to the intersection plane is:

$$d1 = 13249 \text{ mm} \quad (14)$$

corresponding to a step position of the source-detector linear stage Axis n.17:

$$A17 = -252266 \text{ steps} \quad (15)$$

From the information written above (eq. 14 and 15), the thin lens equation (eq. 1) and the setup (fig. 13) we obtained a focal length $f_{MM0027-pixi-fwhm}$ of:

³In the next future laser tracker system will be installed for sub millimeter accuracy measurements.

$$f_{MM0027-pixi-fwhm} = \text{mm} \quad (16)$$

Using the d1 written before and knowing the motor step positions (figures 28), we obtained the value of the focal length for different setup and as function of HEW and xFWHM (table 14).

Table 14: Results of the focus scan, after the mirror alignment. The results are obtained using the 90% mask. The contribution of the source has been subtracted from the xFWHM. In the other case the contribution is negligible.

MM-0027 (XOU-0048): focus search using transversal FWHM (xFWHM)						
MM	Detector	Motor steps 1.25 $\mu\text{m}/\text{step}$	d2 (fig. 11) (mm)	HEW (arcsec)	xFWHM (arcsec)	Focal Length (mm)
MM-0027 XOU-0048	PIXI	-252266	13274 \pm 3 mm	22.5	1.7	11929
	TRoPIC	-235252	13316 \pm 3 mm	26	2	11963

Table 15: Results of the focus scan, after the mirror alignment. The results are obtained using the 90% mask.

MM-0027 (XOU-0048): Focus performances using HEW as focusing parameter						
MM	Detector	Motor steps 1.25 $\mu\text{m}/\text{step}$	d2 (fig. 11) (mm)	HEW (arcsec)	xFWHM (arcsec)	Focal Length (mm)
MM-0027 XOU-0048	PIXI	-391662	13100 \pm 3 mm	22.2	8	11787
	TRoPIC	-302729	13208 \pm 3 mm	26	5	11895

The difference between the focal length obtained with the two detector is probably due the fact that PIXI is not energy sensitive. Reversely TRoPIC has a worse position accuracy. Because of those differences between the two instruments we cannot really prefer one of the two (see section 2.3 for more details). Moreover, for efficiency purpose, the tube settings used with the two detectors are slightly different (table 16).

The focal length obtained using HEW as main parameter is reported in table 15 and it shows a shorter focal length.

Table 16: X-ray tube value set during the MM-0027 focus search with TRoPIC detector.

Detector	Target	Filter	Fluorescence line [7]	kV	Focusing	Heating
TRoPIC	Al	Al	Al-K = 1.486 keV	3	50 V	4.95 V
PIXI	Al	Al	Al-K = 1.486 keV	5	50 V	6.8 V

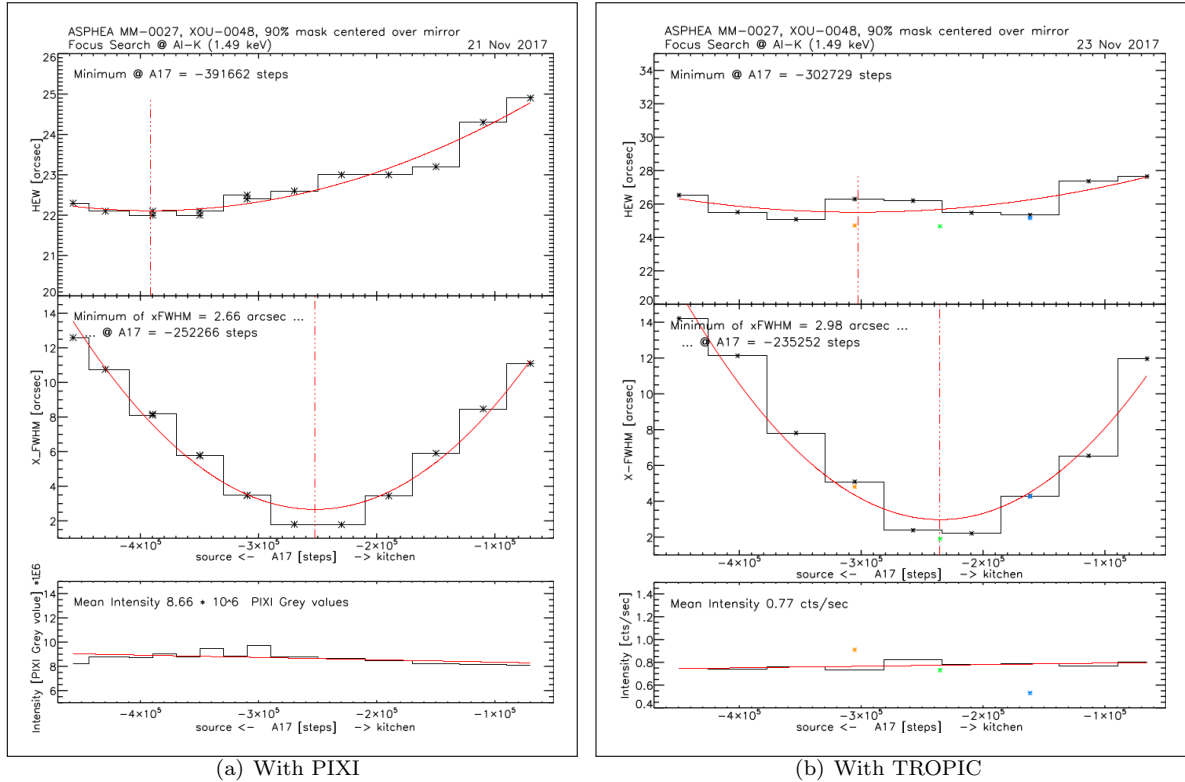


Figure 28: MM-0027 (XOU-0041B) focus search. 90% mask centered over mirror.

9.3 MM-0027: azimuthal scan with PIXI and TROPIC

In this section we report graph and images acquired during the azimuthal scan. It consists in the acquisition of images and flux with a mask that cover only the 5% of the entire mirror module. The aperture is rectangular (see aperture C in figure 15).

Large deformation are visible on the side of the optics itself.

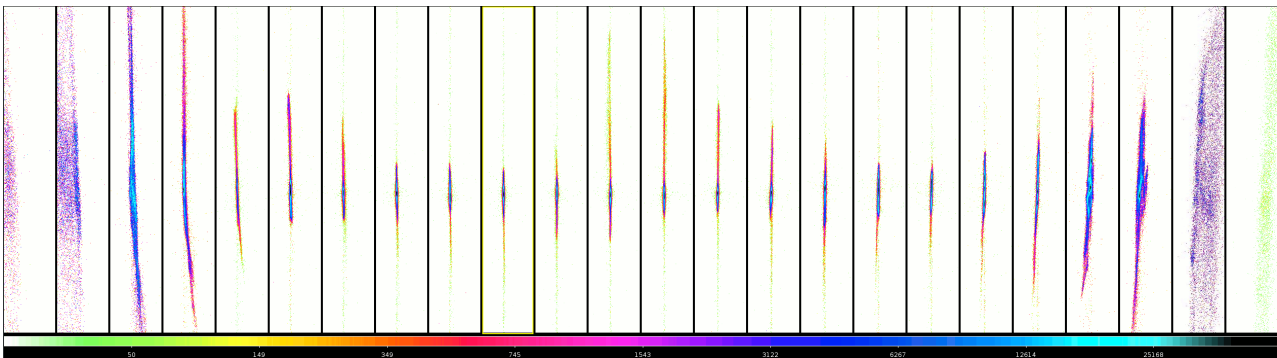


Figure 29: ASPHEA MM-0027, XOU-0048 5% mask Azimuthal Scan with PIXI.

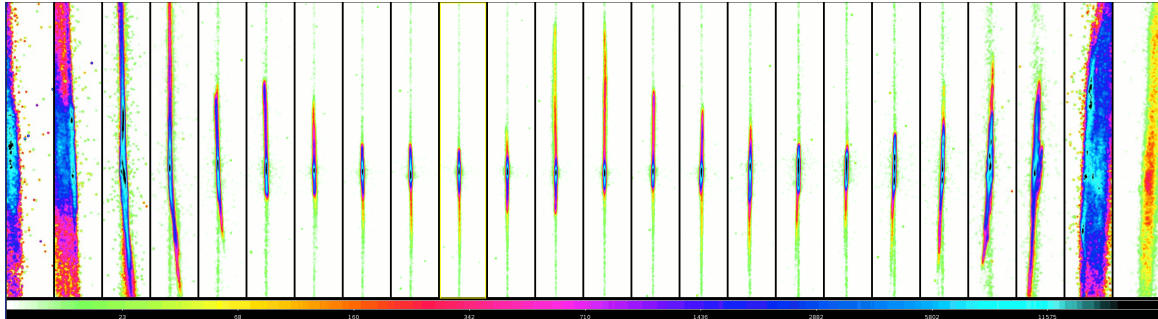


Figure 30: ASPHEA MM-0027, XOU-0048 5% mask Azimuthal Scan with PIXI. Data point are smoothed for best visualization.

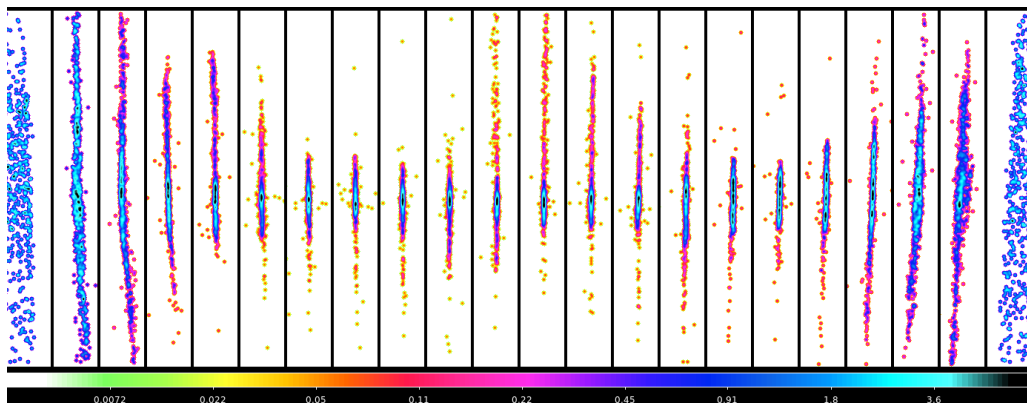


Figure 31: ASPHEA MM-0027, XOU-0048 5% mask Azimuthal Scan with TRoPIC. Data point are smoothed for best visualization.

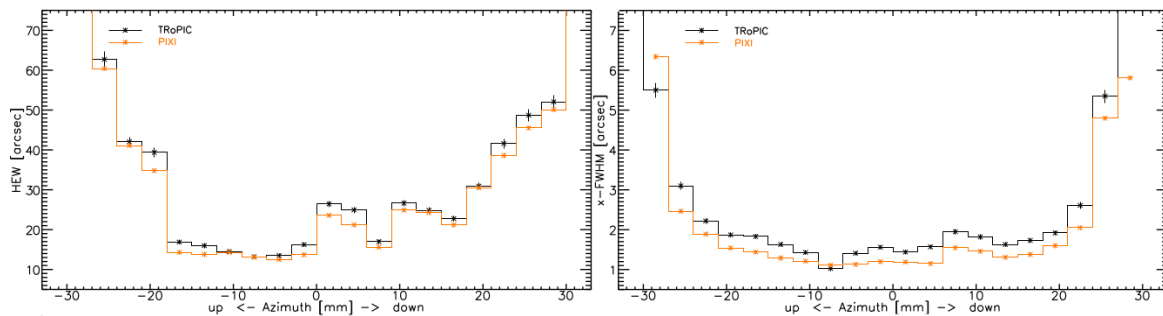


Figure 32: ASPHEA MM-0027, XOU-0048 5% mask Azimuthal Scan with both TRoPIC and PIXI. X-ray tube parameter: Energy line: Al-K, Filter: 10 μm Al, Voltage: 5 kV, Focusing = 50 V; Heating: 6.1 V; in-focus.

10 Results

We summarize the results of the test campaign reporting only the analysis referred to the transversal FWHM that looks to be more reproducible and more easy to measure.

For each mirror we performed:

1. Laser alignment.
2. X-ray alignment: Pitch and Yaw to maximize the flux. In practice is the best alignment of the optics with X-ray beam.
3. Focus scan in order to localize the focus position.
4. Azimuthal scan to analyse the behavior of a small part (5%) of the mirror in radial direction.

Table 17: MM-0025 and MM-0027 pitch and yaw alignment.

Mirror Module	MM-0027			MM-0025		
Detector	PIXI	TRoPIC	(TRoPIC - PIXI)	PIXI	TRoPIC	(TRoPIC - PIXI)
Pitch (arcmin)	+62.085	+62.11	+1.5''	+60.895	+61.34	26.7''
Yaw (arcmin)	-19.300	-19.81	-30''	-21.510	-20.71	-48''

Table 18: Results of the focus scan, after the mirror alignment. The results are obtained using the 90% mask. The contribution of the source has been subtracted from the xFWHM. In the other case the contribution is negligible.

Focus behavior using transversal FWHM (xFWHM) as focusing parameter.						
MM	Detector	Motor steps 1.25 $\mu\text{m}/\text{step}$	d2 (fig. 11) (mm)	HEW arcsec	xFWHM arcsec	Focal length
MM-0025	PIXI	-260515	13288	20.2	1.7	11941
	TRoPIC	-257329	13313	24.3	1.7	11961
	TRoPIC -PIXI					20
MM-0027	PIXI	-252266	13274	22.5	1.7	11929
	TRoPIC	-235252	13316	26.0	2	11963
	TRoPIC -PIXI					34

Table 19: We report the measure distances between PIXI CCD and intersection plane of the optics. Then we calculate the effective focal length using the thin lens equation (equation 1). ip = intersection plane

distance (fig. 11)	Laser (mm)	i (fig. 11) (mm)	f (fig. 10) (mm)
d1 MM-0025	13263	13267	11940
d1 MM-0027	13249	13253	11929



11 Summary

We successfully characterized the XOU-0041b and XOU-0048 respectively mounted in the mirror modules MM-0025 and MM-0027. The results confirm the measurement taken at the BESSY radiation facility during the integration of the modules.

These modules will be used in the ATHENA AIT tests at PANTER in which the co-alignment of two optics module in a mini-petal performed. The mentioned mini-petal is a representative small section of the final ATHENA mirror assembly.

Moreover, after characterizing these two SPO optics provided for the ATHENA AIT efforts we conclude that the quality of the optics is not yet sufficiently good to be used as a “master optic” for the verification of BEaTriX. Further better optics will have to be characterized for the use as a ”master optic” as the optical quality of the SPOs improves during the ongoing development.

The results here show a snapshot of the technology development status in Nov. 2017.



References

- [1] V. Burwitz, M. Bavdaz, G. Pareschi, M. Collon, W. Burkert, D. Spiga, G. Hartner, M. Ackermann, B. Menz, and M. Civitani. In focus measurements of IXO type optics using the new PANTER x-ray test facility extension. *proc. SPIE*, 8861, September 2013.
- [2] K. Dennerl, W. Burkert, V. Burwitz, M. Freyberg, P. Friedrich, and G. Hartner. Determination of the eROSITA mirror half energy width (HEW) with subpixel resolution. *proc. SPIE*, 8443, September 2012.
- [3] S. Ebermayer, R. Andritschke, J. Elbs, N. Meidinger, L. Strüder, R. Hartmann, A. Gottwald, M. Krumrey, and F. Scholze. Quantum efficiency measurements of eROSITA pnCCDs. *proc. SPIE*, 7742, July 2010.
- [4] N. Meidinger, R. Andritschke, S. Ebermayer, J. Elbs, O. Hälker, R. Hartmann, S. Herrmann, N. Kimmel, P. Predehl, G. Schächner, H. Soltau, L. Strüder, and L. Tiedemann. CCD detectors for spectroscopy and imaging of x-rays with the eROSITA space telescope. *proc. SPIE*, 7435, 2009.
- [5] E. Pedersoli, Flavio Capotondi, Daniele Cocco, Marco Zangrando, Burkhard Kaulich, Ralf H. Menk, Andrea Locatelli, Tefvik O. Montes, Carlo Spezzani, Gilio Sandrin, Daniel M. Bacescu, Maya Kiskinova, Saša Bajt, Miriam Barthelmeß, Anton Barty, Joachim Schulz, Lars Gumprecht, Henry N. Chapman, A. J. Nelson, Matthias Frank, Michael J. Pivovarov, Bruce W. Woods, Michael J. Bogan, and Janos Hajdu. Multipurpose modular experimental station for the DiProI beamline of Fermi@Elettra free electron laser. *Review of Scientific Instruments*, 82(4):–, 2011.
- [6] Carlo Pelliciani. AHEAD-WP8-D8.7-D41-ZPC. Technical report, April 2018.
- [7] Albert C. Thompson, Janos Kirz, et al. X-RAY DATA BOOKLET. Univeristy of California, Berkeley, September 2009.